Generalized theory and application of Stokes parameter measurements made with a single photoelastic modulator

Liu, YW, Jones, GA, Peng, Y and Shen, T

http://dx.doi.org/10.1063/1.2353894

Generalized theory and application of Stokes parameter measurements made with a single photoelastic modulator

Yanwei Liu, Grenville A. Jones, Yong Peng, and Tiehan H. Shen[a)]
Joule Physics Laboratory, Institute for Materials Research, University of Salford, Salford M5 4WT, United Kingdom

(Received 6 April 2005; accepted 7 August 2006)

We report in this paper a generalized theory that describes the interaction between a monochromatic light beam and an optical system that includes one photoelastic modulator, one analyzer, and one photodetector. Based on the theory, a detailed four-step procedure is presented, which allows a precise measurement of the four Stokes parameters. An analysis of the systematic and random errors arising from the four-step measurements is also given as well as a calibration procedure that involves the use of a general retardation plate. As a practical application the procedure is used to analyze the magneto-optical properties of magnetic thin films grown on GaAs(001) substrates.
 [DOI: 10.1063/1.2353894]

I. INTRODUCTION

Polarization is a fundamental property of light and changes in the state of polarization of a light beam can provide deep insights into the interaction between light and matter. Accordingly, experimental methods used for the determination of the polarization state are of great interest. In this respect the introduction of the photoelastic modulator (PEM) over the last few decades has been of crucial significance.

The PEM (Ref. 1) is a device that exploits the photoelastic effect to produce a phase retardation with a highly precise sinusoidal time variation, which can be used to modulate the polarization state of a light beam. On account of its high sensitivity, wide spectral range, and high precision phase modulation, the PEM has figured prominently in a wide range of physical measurements.[2–9] In brief, the PEM can be used in any system for which a specified polarization state must be generated or, conversely, for the analysis of the polarization states of any given light beam.

Measuring devices that employ two PEMs have been devised but it remains true that apparatus with a single PEM is still widely used. Although much excellent theoretical and experimental work concerning the determination of polarization states using a single PEM has been reported,[10–14] we believe that a more generalized theory is still very desirable for the full understanding of the measurement procedure (Sec. II) including an analysis of errors (Sec. IV). In Sec. III, a calibration procedure for the entire system is presented, which involves the use of a wave plate of arbitrary retardation and is independent of retardation produced by the PEM, whereas the more usual calibration method requires an exact quarter wave plate corresponding to the light source.

This paper is intended primarily as a study of the principles underlying the use of a single PEM. However, by way of illustrating these principles, we present in Sec. V some magneto-optical data obtained from magnetic thin films. This involves a determination of the Stokes parameters.[15,16] More details on the experimental layout will be found in that section. Suffice it to say here that the theoretical analysis of Secs. II–IV is predicated on a conventional setup that uses a modern PEM together with a lock-in amplifier to measure ac signals and an electrometer to monitor dc signals.

II. THEORETICAL ANALYSIS

For monochromatic or quasimonochromatic light, any given possible polarization state can be represented uniquely by a set of four real quantities, called the Stokes parameters and denoted here as I, Q, U, and V. They are defined as follows:[15,16]

$$\begin{aligned} I &= I_{0^\circ} + I_{90^\circ} = I_{45^\circ} + I_{-45^\circ}, \\ Q &= I_{0^\circ} - I_{90^\circ}, \\ U &= I_{45^\circ} - I_{-45^\circ}, \\ V &= I_{\mathrm{LC}} - I_{\mathrm{RC}}. \end{aligned} \tag{1}$$

Here, I is the total intensity, Q is the difference in intensities between light passing through horizontally and vertically aligned linear polarizers, U is the difference in intensities between linear polarizers at +45° and −45°, and V is the difference in intensities between right and left circularly polarized components. For the case of quasimonochromatic light, the parameters must be time averaged. The advantage of working with the Stokes parameters is that they may be used to describe partially polarized light. Depolarization may occur as a result of interaction of the light with a medium either in reflection or transmission.

The following relationship exists between the Stokes parameters, namely,

$$I^2 \geqslant Q^2 + U^2 + V^2. \tag{2}$$

The equality holds for fully (100%) polarized light and the inequality pertains to partially polarized light.

We now present the theory for the general case of a monochromatic light beam of arbitrary polarization (whose

[a)]Author to whom correspondence should be addressed; FAX: +44-161-2955575; electronic mail: t.shen@salford.ac.uk

state is to be determined) transmitted at normal incidence firstly through a PEM and then through an analyzer (A) before striking a photodetector. The angular disposition of the components is shown in Fig. 1.

Following modern practice we shall use Müller matrices to describe the interaction between the light and the optical devices as they may be used to describe a partially polarized light.

The Müller matrix for the PEM can be written as follows:[17]

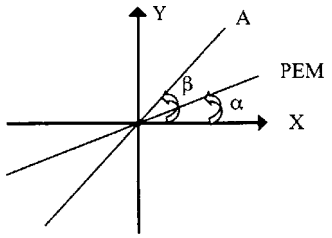

FIG. 1. Orientation of PEM and analyzer (A) relative to x axis (laboratory coordinate): α is the angle between the fast axis of the PEM and the x axis and β is the angle between the passing axis of the analyzer and the x axis.

$$M_1 = \begin{pmatrix} 1 & 0 & 0 & 0 \\ 0 & \cos(4\alpha)\sin^2(\delta/2) + \cos^2(\delta/2) & \sin(4\alpha)\sin^2(\delta/2) & -\sin(2\alpha)\sin(\delta) \\ 0 & \sin(4\alpha)\sin^2(\delta/2) & -\cos(4\alpha)\sin^2(\delta/2) + \cos^2(\delta/2) & \cos(2\alpha)\sin(\delta) \\ 0 & \sin(2\alpha)\sin(\delta) & -\cos(2\alpha)\sin(\delta) & \cos(\delta) \end{pmatrix}. \tag{3a}$$

Here, $\delta = \delta_0 \sin(\Omega t)$ is the retardation produced by the PEM, δ_0 is the amplitude of the retardation, and Ω is the modulating frequency of the PEM.

Similarly for the analyzer, the Müller matrix is written as[17]

$$M_2 = \frac{1}{2}\begin{pmatrix} 1 & \cos(2\beta) & \sin(2\beta) & 0 \\ \cos(2\beta) & \cos^2(2\beta) & \cos(2\beta)\sin(2\beta) & 0 \\ \sin(2\beta) & \cos(2\beta)\sin(2\beta) & \sin^2(2\beta) & 0 \\ 0 & 0 & 0 & 0 \end{pmatrix}. \tag{3b}$$

Using these matrices we get the following relation:

$$\begin{pmatrix} I' \\ Q' \\ U' \\ V' \end{pmatrix} = M_2 M_1 \begin{pmatrix} I \\ Q \\ U \\ V \end{pmatrix}, \tag{4}$$

where $(I\ Q\ U\ V)^T$ and $(I'\ Q'\ U'\ V')^T$ are the Stokes vectors of the light entering the PEM (whose state is to be determined) and the photodetector, respectively. The photodetector measures only the first Stokes parameter I', a fact that greatly simplifies the algebra. Multiplying out Eq. (4) we get

$$\begin{aligned} I' = {} & \tfrac{1}{2}I + \tfrac{1}{2}Q\cos(2\beta - 2\alpha)\cos(2\alpha) + \tfrac{1}{2}U\cos(2\beta \\ & - 2\alpha)\sin(2\alpha) \\ & - \tfrac{1}{2}Q\sin(2\beta - 2\alpha)\sin(2\alpha)\cos(\delta) \\ & + \tfrac{1}{2}U\sin(2\beta - 2\alpha)\cos(2\alpha)\cos(\delta) \\ & + \tfrac{1}{2}V\sin(2\beta - 2\alpha)\sin(\delta). \end{aligned} \tag{5}$$

In view of the lock-in technique employed, we further expand the retardation in terms of Bessel functions to get the Fourier components. The standard expansions are

$$\begin{aligned} \sin(\delta) &= \sin[\delta_0 \sin(\Omega t)] \\ &= 2J_1(\delta_0)\sin(\Omega t) + 2J_3(\delta_0)\sin(3\Omega t) + \cdots, \end{aligned} \tag{6}$$

$$\begin{aligned} \cos(\delta) &= \cos[\delta_0 \sin(\Omega t)] \\ &= J_0(\delta_0) + 2J_2(\delta_0)\cos(2\Omega t) + 2J_4(\delta_0)\cos(4\Omega t) + \cdots. \end{aligned} \tag{7}$$

Using Eqs. (6) and (7), we may rewrite Eq. (5) as

$$\begin{aligned} I' = {} & \tfrac{1}{2}I + \tfrac{1}{2}Q\cos(2\beta - 2\alpha)\cos 2\alpha + \tfrac{1}{2}U\cos(2\beta - 2\alpha)\sin(2\alpha) \\ & - \tfrac{1}{2}J_0(\delta_0)Q\sin(2\beta - 2\alpha)\sin(2\alpha) \\ & + \tfrac{1}{2}J_0(\delta_0)U\sin(2\beta - 2\alpha)\cos(2\alpha) \\ & + J_1(\delta_0)V\sin(2\beta - 2\alpha)\sin(\Omega t) \\ & - J_2(\delta_0)Q\sin(2\beta - 2\alpha)\sin(2\alpha)\cos(2\Omega t) \\ & + J_2(\delta_0)U\sin(2\beta - 2\alpha)\cos(2\alpha)\cos(2\Omega t) + \cdots. \end{aligned} \tag{8}$$

The terms of the equation have been arranged to reflect the magnitudes of the dc (second line) signal and the first (F) (third line) and second ($2F$) (fifth line) harmonic signals. From Eq. (8), it is seen that all these low Fourier components are strongly dependent on the orientations of the two optical components as well as the amplitude of the retardation produced by the PEM. The extraction of the four Stokes parameters is thus not a simple task. In fact, traditional methods to measure the Stokes parameters (using an analyzer and a quarter wave plate) normally involve six distinct settings of components[15,16] but here we present a procedure that uses only four. Inspection of Eq. (8) shows that obvious choices

AQ: #1

AQ: #2

AQ: #3

of settings are as follows: setting (1) $\alpha=0°$, $\beta=45°$; setting (2) $\alpha=0°$, $\beta=-45°$; setting (3) $\alpha=45°$, $\beta=0°$; and setting (4) $\alpha=45°$, $\beta=90°$.

It should be noted that an angle of 45° is maintained between the two components for all the settings; this maximizes the F and $2F$ signals. Angles of $\alpha=0°$ and 45° are chosen in order to measure separately U and Q. By way of illustration, consider setting (1). Using Eq. (8) we have

$$I' = \tfrac{1}{2}I + \tfrac{1}{2}J_0(\delta_0)U + J_1(\delta_0)V\sin(\Omega t) + J_2(\delta_0)U\cos(2\Omega t) + \cdots, \tag{9}$$

from which we derive the following signals:

AQ: #4

Setting (1),

$$I_{dc}(0°,45°) = \tfrac{1}{2}I + \tfrac{1}{2}J_0(\delta_0)U,$$
$$I_F(0°,45°) = \frac{\sqrt{2}}{2}J_1(\delta_0)V, \tag{10}$$
$$I_{2F}(0°,45°) = \frac{\sqrt{2}}{2}J_2(\delta_0)U,$$

where, in an obvious notation, $I_{dc}(0°,45°)$, $I_F(0°,45°)$, and $I_{2F}(0°,45°)$, respectively, represent the dc [first line of Eq. (9)], F [second line of Eq. (9)], and $2F$ [third line of Eq. (9)] signal obtained in setting (1). The factor $\sqrt{2}/2$ comes from the rms value detected by the lock-in amplifier.

A similar procedure yields expressions analogous to Eq. (10) for the three other settings;

Setting (2),

$$I_{dc}(0°,-45°) = \tfrac{1}{2}I - \tfrac{1}{2}J_0(\delta_0)U,$$
$$I_F(0°,-45°) = \frac{\sqrt{2}}{2}J_1(\delta_0)V, \tag{11}$$
$$I_{2F}(0°,-45°) = \frac{\sqrt{2}}{2}J_2(\delta_0)U.$$

Setting (3),

$$I_{dc}(45°,0°) = \tfrac{1}{2}I + \tfrac{1}{2}J_0(\delta_0)Q,$$
$$I_F(45°,0°) = \frac{\sqrt{2}}{2}J_1(\delta_0)V, \tag{12}$$
$$I_{2F}(45°,0°) = \frac{\sqrt{2}}{2}J_2(\delta_0)Q.$$

Setting (4),

$$I_{dc}(45°,90°) = \tfrac{1}{2}I - \tfrac{1}{2}J_0(\delta_0)Q,$$
$$I_F(45°,90°) = \frac{\sqrt{2}}{2}J_1(\delta_0)V, \tag{13}$$
$$I_{2F}(45°,90°) = \frac{\sqrt{2}}{2}J_2(\delta_0)Q.$$

TABLE I. The measurements needed to deduce any given Stokes parameters.

Stokes parameter	Measurements needed to deduce the Stokes parameter
I	$I_{dc}(0°,45°)$ and $I_{dc}(0°,-45°)$ or $I_{dc}(45°,0°)$ and $I_{dc}(45°,90°)$
Q	$I_{2F}(45°,0°)$ or $I_{2F}(45°,90°)$
U	$I_{2F}(0°,45°)$ or $I_{2F}(0°,-45°)$
V	$I_F(0°,45°)$, $I_F(0°,-45°)$, $I_F(45°,0°)$, or $I_F(45°,90°)$

The significance of these equations can be grasped more readily by reference to Table I which shows the signals required to determine any given Stokes parameter. Two points are of interest: (i) a combination of two settings is required to determine I whereas a single (but not necessarily the same) setting suffices to find V, U, and Q; (ii) a minimum of five signals only [e.g., $I_{dc}(0°,45°)$, $I_{dc}(0°,-45°)$, $I_F(0°,45°)$, $I_{2F}(0°,45°)$, and $I_{2F}(45°,0°)$] is required in order to make a complete determination of the Stokes parameters. This can be accomplished using just three settings [in this case (1), (2), and (3)].

The information contained in Eqs. (10)–(13) may be rewritten in the form

AQ: #5

$$\begin{aligned} I &= I_{dc}(0°,45°) + I_{dc}(0°,-45°) \\ &= I_{dc}(45°,0°) + I_{dc}(45°,90°) \\ &= \tfrac{1}{2}[I_{dc}(0°,45°) + I_{dc}(0°,-45°) \\ &\quad + I_{dc}(45°,0°) + I_{dc}(45°,90°)], \\ Q &= k_2 I_{2F}(45°,0°) \\ &= k_2 I_{2F}(45°,90°) \\ &= \tfrac{1}{2}k_2[I_{2F}(45°,0°) + I_{2F}(45°,90°)], \\ U &= k_2 I_{2F}(0°,45°) \\ &= k_2 I_{2F}(0°,-45°) \\ &= \tfrac{1}{2}k_2[I_{2F}(0°,45°) + I_{2F}(0°,-45°)], \\ V &= k_1 I_F(0°,45°) \\ &= k_1 I_F(0°,-45°) \\ &= k_1 I_F(45°,0°) \\ &= k_1 I_F(45°,90°) \\ &= \tfrac{1}{4}k_1[I_F(0°,45°) + I_F(0°,-45°) + I_F(45°,0°) \\ &\quad + I_F(45°,90°)]. \end{aligned} \tag{14}$$

Here $k_1=\sqrt{2}/J_1(\delta_0)$ and $k_2=\sqrt{2}/J_2(\delta_0)$ are constants whose values must be determined (Sec. III). All 12 signals have been incorporated into Eq. (14) but many of the configurations are equivalent. Our practice is to measure all signals at the outset of the experiment because they serve as a check of internal consistency. If it becomes clear that the system is well behaved then the number of components measured can be reduced. The greatest deviation amongst

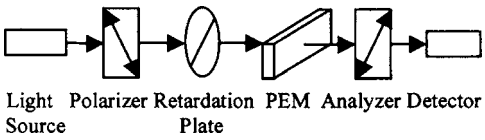

FIG. 2. Experimental setup for calibration of the system.

equivalent signals is found during the measurements of U and Q particularly if either quantity is relatively very small.

Once the constants k_1 and k_2 are known, the four Stokes parameters can be calculated from Eq. (14). Knowledge of the Stokes parameters now allows an alternative description of the polarization state in terms of the five ellipsometric parameters:[11,15–17]

(1) The orientation of the polarized light,

$$\psi = \frac{1}{2}\tan^{-1}\left(\frac{U}{Q}\right). \tag{15}$$

(2) The ellipticity angle,[18]

$$\chi = \frac{1}{2}\sin^{-1}\left(\frac{V}{\sqrt{Q^2+U^2+V^2}}\right). \tag{16}$$

(3) The degree of total polarization,

$$P = \frac{\sqrt{Q^2+U^2+V^2}}{I}. \tag{17}$$

(4) The degree of linear polarization,

$$P_L = \frac{\sqrt{Q^2+U^2}}{I}. \tag{18}$$

(5) The degree of circular polarization,

$$P_C = \frac{V}{I}. \tag{19}$$

These five parameters may be expressed in terms of the experimental measurements using Eq. (14).

III. CALIBRATION

In principle, the constants k_1 and k_2 could be computed directly from the Bessel functions but this involves the assumption that the retardation amplitude δ_0 is known precisely and that the lock-in amplifier has an ideal performance (i.e., the gain is unity and independent of input amplitude and frequency). For these reasons a calibration of the entire optical system is preferable. Below we outline a general calibration procedure that uses a wave plate of arbitrary retardation.

The setup is shown in Fig. 2. The passing axis of the polarizer is set at 0° (denoted as the x axis of the laboratory coordinate system) and the analyzer rotated to the extinction position. The PEM is now inserted into the light path and slowly rotated until an extinction of the $2F$ signal (or dc signal) is observed. This corresponds to the fast axis (or slow axis) of the PEM lying parallel to the x axis. In view of the importance of this reference axis, it may be checked as follows. The passing axis of the polarizer is set at a series of

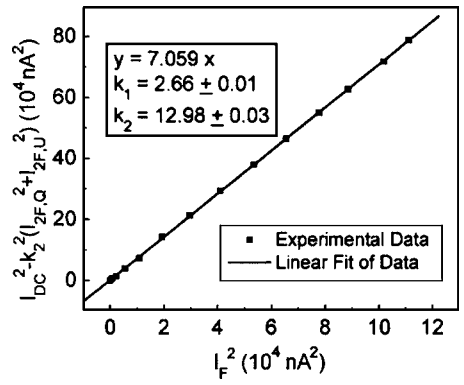

FIG. 3. Calibration curve of the measurement system with a retardation plate. The nominal retardation amplitude of the PEM is 0.414λ.

angles (e.g., 5°, 10°, and 15°) with respect to the x axis and all the $2F$ signals $[I_{2F}(0°,45°), I_{2F}(0°,-45°), I_{2F}(45°,0°)$, and $I_{2F}(45°,90°)]$ for each position are measured. The orientation of the linearly polarized light can now be calculated for each position—using Eqs. (14) and (15)—and compared with the preset values. When our system is well aligned any deviation in excess of 0.05° may be taken as an indication of maladjustment. Once the position of the fast axis of the PEM is well defined, the retardation plate is now put into the calibration system (see Fig. 2). The light emerging from the plate is 100% elliptically polarized. Accordingly, the equality (2) holds and combined with Eq. (14) yields

$$\begin{aligned}&[I_{\mathrm{dc}}(0°,45°)+I_{\mathrm{dc}}(0°,-45°)+I_{\mathrm{dc}}(45°,0°)\\&\quad+I_{\mathrm{dc}}(45°,90°)]\\&=k_2^2\{[I_{2F}(0°,45°)+I_{2F}(0°,-45°)]+[I_{2F}(45°,0°)\\&\quad+I_{2F}(45°,90°)]\}+\tfrac{1}{4}k_1^2[I_F(0°,45°)+I_F(0°,-45°)\\&\quad+I_F(45°,0°)+I_F(45°,90°)].\end{aligned} \tag{20}$$

The plate is now rotated about the optic axis in small-angle increments. The state of (elliptical) polarization changes at each angular position: these changes can be monitored by measurement of all the dc, F, and $2F$ signals pertinent to that orientation. Finally, the series of data so acquired is fitted to Eq. (20), thus leading to the simultaneous determination of the coefficients k_1 and k_2. Figure 3 shows the calibration curve obtained in this way for our system. The data points give an excellent linear fit thus proving the efficacy of the technique.

The above calibration procedure does not require an exact quarter wave plate corresponding to the light source, and there is no need to know the actual values of the retardations provided by the PEM and the retardation plate. However, if such an exact quarter wave plate is available the calibration can be done more quickly. Without the plate in the system the light entering the PEM (Fig. 2) is 100% linearly polarized and the coefficient k_2 can be found by combining Eqs. (14) and (18). If the quarter wave plate is inserted and set at the correct azimuthal angle, a pure circularly polarized light is produced: the coefficient k_1 can be obtained by combining Eqs. (14) and (19). The constants k_1 and k_2 are strongly

dependent on the amplitude of the retardation generated by the PEM and the system must be recalibrated if δ_0 is changed.

IV. SYSTEMATIC AND RANDOM ERRORS

Many factors may introduce errors, both random and systematic, into the determination of the Stokes parameter measurements using the PEM technique. These are discussed briefly below.

Misalignment of the optical system is an obvious source of systematic error. In particular, we have found it essential to ensure that the emergent light strikes the same area of the photodiode detector regardless of the azimuthal settings of the optical components. Unfortunately, this misalignment cannot be completely eliminated in our experimental system. This accounts for an error of about 1%. The retardation amplitude and the residual (static) birefringence of the PEM should also be considered as possible sources of systematic error. The accuracy of the retardation amplitude is crucial for the Stokes parameter measurement if direct calculation of the Bessel functions is attempted. However, the value of δ_0 becomes irrelevant if the calibration procedures outlined above are used; any influence of δ_0 is already contained in the coefficients k_1 and k_2, whose values can be determined to an accuracy of better than 0.5%. A sizable residual birefringence in the PEM can cause problems[12,14] because the optical system can no longer be set to preferred configurations in order to obtain separate measurements of I, Q, U, and V. Fortunately, extensive tests on our device show that the phase retardation associated with its residual birefringence is very small ($<0.015°$) and thus negligible compared with other errors.

Fluctuations in the intensity of the incident light are a potential source of random error, albeit small; after a warm-up period of 1 h the laser used in this work is stable to within 0.3%. The retardation amplitude δ_0 may also be susceptible to a random fluctuation (as opposed to a systematic offset) but we have no means of testing this possibility. Other errors may be specific to a particular application, e.g., the instability of the magnetic field in magneto-optical measurements (Sec. V). Irrespective of application, the setting of the optical components for any of the four configurations will be subject to a random error in the azimuthal angles. However, once their positions are fixed, the error becomes systematic for all the measurements taken within that configuration. We now discuss the implications of such errors on the measurement of the Stokes parameters for an ideal case in which the light intensity is highly stable, the optical alignment is perfect, and the PEM has no measurable residual birefringence.

Let ε_1 and ε_2 represent the maximal deviations from the ideal azimuthal settings of the PEM and analyzer. If we consider the first step ($\alpha=0°$; $\beta=45°$) as an example then, after incorporating the setting errors, Eq. (8) becomes

$$\begin{aligned} I' = {} & \tfrac{1}{2}I - \tfrac{1}{2}Q\sin(2\varepsilon_2 - 2\varepsilon_1)\cos(2\varepsilon_1) \\ & - \tfrac{1}{2}U\sin(2\varepsilon_2 - 2\varepsilon_1)\sin(2\varepsilon_1) \\ & - \tfrac{1}{2}J_0(\delta_0)Q\cos(2\varepsilon_2 - 2\varepsilon_1)\sin(2\varepsilon_1) \\ & + \tfrac{1}{2}J_0(\delta_0)U\cos(2\varepsilon_2 - 2\varepsilon_1)\cos(2\varepsilon_1) \\ & + J_1(\delta_0)V\cos(2\varepsilon_2 - 2\varepsilon_1)\sin(\Omega t) \\ & - J_2(\delta_0)Q\cos(2\varepsilon_2 - 2\varepsilon_1)\sin(2\varepsilon_1)\cos(2\Omega t) \\ & + J_2(\delta_0)U\cos(2\varepsilon_2 - 2\varepsilon_1)\cos(2\varepsilon_1)\cos(2\Omega t) + \cdots . \end{aligned} \tag{21}$$

In our system the absolute values of ε_1 and ε_2 are of the same order of magnitude and so we put $|\varepsilon_1|=|\varepsilon_2|=\varepsilon$. Compared with Eq. (10) for the error-free configuration, the maximum experimental errors for the dc [second line Eq. (21)], $2F$ [fifth line Eq. (21)], and F [third line of Eq. (21)] components can be written as follows:

$$\begin{aligned} \Delta I_{\mathrm{dc}}(0°,45°) &\cong \tfrac{1}{2}Q\sin(4\varepsilon)\cos(2\varepsilon) + \tfrac{1}{2}U\sin(4\varepsilon)\sin(2\varepsilon) \\ &\quad + \tfrac{1}{2}J_0(\delta_0)Q\cos(4\varepsilon)\sin(2\varepsilon) \\ &\cong 2\varepsilon Q + J_0(\delta_0)\varepsilon Q, \\ \Delta I_F(0°,45°) &\cong \frac{\sqrt{2}}{2}J_1(\delta_0)V[1-\cos(4\varepsilon)] \\ &\cong 4\sqrt{2}J_1(\delta_0)\varepsilon^2 V, \\ \Delta I_{2F}(0°,45°) &\cong \frac{\sqrt{2}}{2}J_2(\delta_0)Q\cos(4\varepsilon)\sin(2\varepsilon) \\ &\cong \sqrt{2}J_2(\delta_0)\varepsilon Q. \end{aligned} \tag{22}$$

It may easily be shown that Eq. (22) is also valid for the second setting ($\alpha=0°$, $\beta=-45°$).

For the third or fourth step, the resulting maximal errors are

$$\begin{aligned} \Delta I_{\mathrm{dc}}(45°,0°) &\cong \tfrac{1}{2}Q\sin(4\varepsilon)\sin(2\varepsilon) + \tfrac{1}{2}U\sin(4\varepsilon)\cos(2\varepsilon) \\ &\quad + \tfrac{1}{2}J_0(\delta_0)U\cos(4\varepsilon)\sin(2\varepsilon) \\ &\cong 2\varepsilon U + J_0(\delta_0)\varepsilon U, \\ \Delta I_F(45°,0°) &\cong \frac{\sqrt{2}}{2}J_1(\delta_0)V[1-\cos(4\varepsilon)] \\ &\cong 4\sqrt{2}J_1(\delta_0)\varepsilon^2 V, \\ \Delta I_{2F}(45°,0°) &\cong \frac{\sqrt{2}}{2}J_2(\delta_0)U\cos(4\varepsilon)\sin(2\varepsilon) \\ &\cong \sqrt{2}J_2(\delta_0)\varepsilon U. \end{aligned} \tag{23}$$

Using Eqs. (22) and (23), we may now deduce the relative errors in the measurement of any given Stokes parameter due to the offset of optical components, namely,

$$\frac{\Delta I}{I} = \frac{\Delta I_{\mathrm{dc}}(0°,45°) + \Delta I_{\mathrm{dc}}(0°,-45°) + \Delta I_{\mathrm{dc}}(45°,0°) + \Delta I_{\mathrm{dc}}(45°,90°)}{I_{\mathrm{dc}}(0°,45°) + I_{\mathrm{dc}}(0°,-45°) + I_{\mathrm{dc}}(45°,0°) + I_{\mathrm{dc}}(45°,90°)} \cong [2 + J_0(\delta_0)]\varepsilon\frac{Q+U}{I} \cong 4\varepsilon,$$

$$\frac{\Delta Q}{Q} \cong \frac{\Delta I_{2F}(45°,0°)}{I_{2F}(45°,0°)} \cong 2\varepsilon\frac{U}{Q},$$

$$\frac{\Delta U}{U} \cong \frac{\Delta I_{2F}(0°,45°)}{I_{2F}(0°,45°)} \cong 2\varepsilon\frac{Q}{U}, \tag{24}$$

$$\frac{\Delta V}{V} \cong \frac{\Delta I_F(0°,45°)}{I_F(0°,45°)} \cong 4\sqrt{2}J_1(\delta_0)\varepsilon^2 \cong 0.$$

It is clear that the relative errors in the Stokes parameter measurements are proportional to ε (or ε^2 in the case of $\Delta V/V$) when ε is a small angle (we estimate ε as 0.03°, equivalent to 5×10^{-4} rad). It may be concluded therefore that incorrect settings of optical components will have negligible effect on I and V. However, Eq. (24) also shows that it is impossible to attain simultaneously small $\Delta Q/Q$ and $\Delta U/U$ if U and Q have widely dispersed values. The ideal condition pertains when $U=Q$. Extreme values of U and Q ($U \gg Q$ and vice versa) have serious implications for errors in ψ [see Eq. (15)] and such situations should be avoided if possible in any real application. If experiments are carried out under the condition, say, $0.2 \leqslant 1U/Q$, then errors arising, $5 \leqslant 1$, from incorrect azimuthal settings will be smaller than 0.5% in our optical system.

The calibration procedure (Sec. III) affords an opportunity of checking Eq. (24) because the values of the Stokes parameters change significantly as the retardation plate is rotated. The spread in measurements of the 12 basic signals for each setting of the plate does confirm the error analysis.

V. EXPERIMENT

In order to test the performance of the four-step measurement procedure we have investigated the magneto-optical properties of magnetic thin films using a reflective geometry. By monitoring the Stokes parameters as a function of magnetic field H, we are able to determine the magneto-optical properties of these magnetic thin films. The experiments were conducted shortly after the calibration procedure.

A. Longitudinal Kerr effect

The sample used in the longitudinal magneto-optical Kerr effect (MOKE) geometry was an epitaxial 3.2 nm Fe film capped with a 1.0 nm Ir protection layer grown on a GaAs(001) substrate in an ultrahigh vacuum molecular beam epitaxy (MBE) system. The experimental setup used in this geometry is shown in Fig. 4. The light beam from a diode laser (Laser 2000, 3 mW, 670 nm) firstly passes through a polarizer to provide a preset linear polarization state and then strikes the sample positioned in the gap center of an electromagnet whose field is parallel to the sample surface. After interaction with the sample with an in-plane magnetic field, the reflected light passes sequentially through a PEM (Hinds Instruments, $f=42$ kHz), an analyzer, and finally a Si photodiode detector. The first (F) and second ($2F$) harmonic components of the signal from the photodiode are measured with a lock-in amplifier (Perkin Elmer 7265) with the PEM modulation frequency as reference and the dc component is measured using a high-precision Keithley 6517 electrometer. The

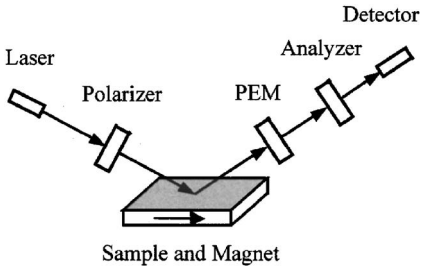

FIG. 4. Setup for studying the magneto-optical Kerr effect of thin films in longitudinal geometry.

polarizers (Karl Lambrecht Corporation Glan-Thompson prisms) have an extinction coefficient better than 1×10^{-6}.

Figure 5 shows the in-plane anisotropy measurements of Kerr rotation and ellipticity angles for this epitaxially grown ultrathin Fe film when the external magnetic field is applied along the four major substrate orientations [110], [100], [010], and [1$\bar{1}$0], respectively. It can be seen that both Kerr rotation angle and ellipticity angle hysteresis loops show an in-plane uniaxial magnetic anisotropy with [110] as easy axis, [1$\bar{1}$0] as hard axis, and [100] and [010] as two equivalent intermediate axes. This is in agreement with the findings of Krebs *et al.*[19] It is also important to note that both the Kerr rotation angle and ellipticity angle hysteresis loops give exactly the same coercivity and same shape in each case.

AQ: #8

B. Polar Kerr effect

The test sample used in the polar MOKE geometry was a Ni film with a nominal thickness of 8.0 nm grown on a GaAs(001) surface which has an off cut angle of 3° towards a [111] direction and is described as "vicinal GaAs(001)." The setup used in this geometry is identical to that of Fig. 4, except that the magnetic field is applied perpendicular to the sample surface and it is near normal incidence.

Figure 6 shows the measurements of Kerr rotation angle and ellipticity angle for this sample in polar MOKE geometry. Clear hysteresis loops are observed in both polar Kerr rotation and ellipticity angle measurements, whereas no such loops have been found from Ni films of the same thickness grown on perfectly flat GaAs(001) surfaces, commonly known as "singular GaAs(001)," at room temperature. This finding seems to indicate that the steps existing on the vicinal substrate surface modify the shape anisotropy and favor an out-of-plane magnetization. Perpendicular magnetic anisotropy in Ni/GaAs(001) has been observed by Haque *et al.*[20] using ferromagnetic resonance (FMR) and a superconducting quantum interference device (SQUID). They found that the magnetic anisotropy was out of plane when the thickness of the Ni film was smaller than 12 nm and became in plane when the thickness was greater than 15 nm. Bakerschke and Farle have also reported a change of sign in the anisotropy of a Ni/Cu(001) system when the thickness of Ni exceeds seven monolayers.[21]

Figure 6 shows that both the Kerr rotation angle and ellipticity angle hysteresis loops give exactly the same coercivity although the shapes of the two loops are different. At the moment we are not clear about the cause of the differ-

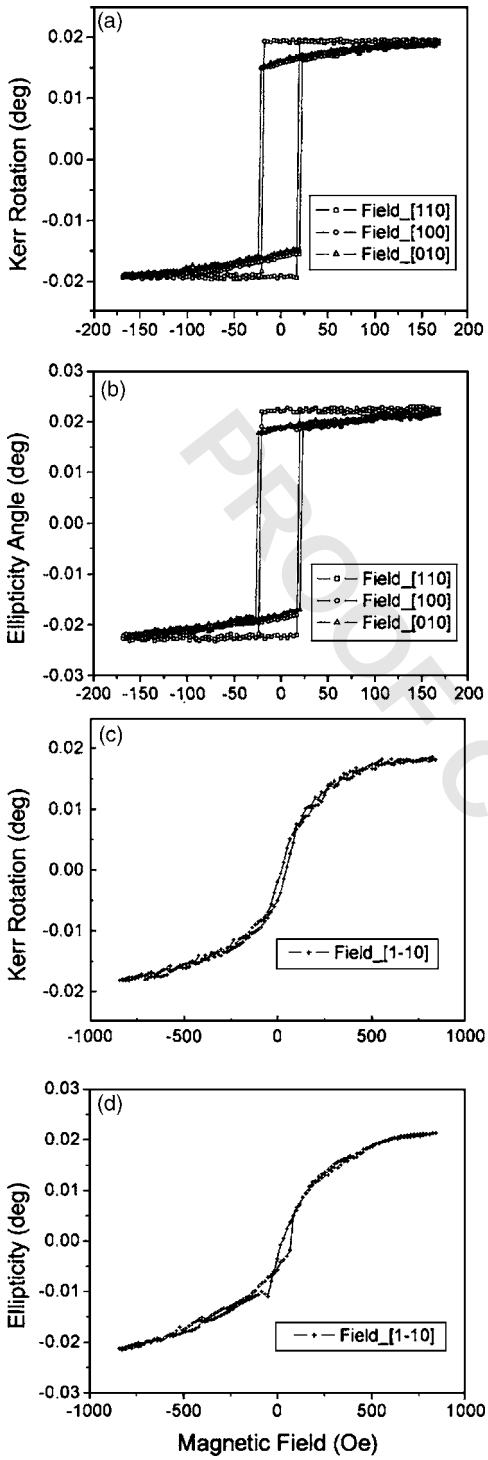

FIG. 5. Dependence of the Kerr rotation angle and ellipticity angle of Ir(1.0 nm)/Fe(3.2 nm)/GaAs on the magnetic field in longitudinal MOKE geometry. The field is applied along [110] (open squares), along [100] (open circles), along [0101] (open triangles), and [$1\bar{1}0$] (crosses). (a) and (c) show Kerr rotation angle while (b) and (d) represent Kerr ellipticity angle.

ence. One possible origin may be attributed to the fact that the magnetization of the thin Ni film used in this measurement is only tilted out of plane but not exactly perpendicular to the sample surface.[22] The applied field is not strong enough to enable the saturation behavior to be observed.

The results shown in Figs. 5 and 6 are ample justification for the validity of the four-step procedure used to determine the magneto-optical properties of thin magnetic films arising

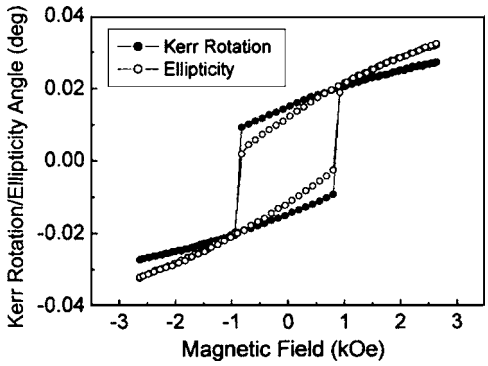

FIG. 6. Dependence of the Kerr rotation and ellipticity angles of Ni(8.0 nm)/GaAs on the magnetic field in polar MOKE geometry. The filled circles are for Kerr rotation angle while the open circles represent Kerr ellipticity angle.

from a reflective (Kerr) geometry. However, the general procedure, as described above, may also be used to analyze the magneto-optical properties obtained in a transmissive (Faraday) geometry. In this respect, we are particularly interested in the properties of nanowire arrays for which case some preliminary results have already been presented.[9]

ACKNOWLEDGMENTS

The authors would like to acknowledge the support of EPSRC and an award from Salford University Research Investment Fund. One of the authors (Y.W.L.) wishes to thank the University of Salford for a Research Studentship.

[1] J. C. Kemp, J. Opt. Soc. Am. **59**, 950 (1969).
[2] J. C. Kemp, G. D. Henson, C. T. Steiner, and E. R. Powell, Nature (London) **326**, 270 (1987).
[3] W. S. Kim, M. Aderholz, and W. Kleemann, Meas. Sci. Technol. **4**, 1275 (1993).
[4] S. N. Jasperson and S. E. Schnatterly, Rev. Sci. Instrum. **40**, 761 (1969).
[5] Y. Shindo and M. Nakagawa, Rev. Sci. Instrum. **56**, 32 (1985).
[6] H. Wang, D. K. Graff, J. R. Schoonover, and R. A. Palmer, Appl. Spectrosc. **53**, 687 (1999).
[7] B. Wang and T. C. Oakberg, Rev. Sci. Instrum. **70**, 3847 (1999).
[8] H. J. Zhu, M. Ramsteiner, H. Kostial, M. Wassermeier, H.-P. Schönherr, and K. H. Ploog, Phys. Rev. Lett. **87**, 016601 (2001).
[9] Y. Peng, T.-H. Shen, B. Ashworth, X.-G. Zhao, C. A. Faunce, and Y.-W. Liu, Appl. Phys. Lett. **83**, 362 (2003).
[10] J. C. Kemp, *Polarized Light and its Interaction with Modulating Devices: A Methodology Review* (Hinds Instrument Inc., ■, 1987). AQ:
[11] T. C. Oakberg, *Stokes Polarimetry* (Hinds Instrument Inc., ■, ■). #9
[12] F. A. Modine, G. E. Jellison Jr., and G. R. Gruzalski, J. Opt. Soc. Am. **73**, 892 (1983). AQ:
[13] E. Compain and B. Drevillon, Rev. Sci. Instrum. **69**, 1574 (1998). #10
[14] J. Badoz, M. P. Silverman, and J. C. Canit, J. Opt. Soc. Am. A **7**, 672 (1990).
[15] R. M. A. Azzam and N. M. Bashara, *Ellipsometry and Polarized Light* (North-Holland, New York, 1977).
[16] M. Born and E. Wolf, *Principles of Optics*, 6th ed. (Pergamon, Oxford, 1980).
[17] D. S. Kliger, J. W. Lewis, and C. E. Randall, *Polarized Light in Optics and Spectroscopy* (Academic, New York, 1990).
[18] In the literature, the terms of ellipticity and ellipticity angle sometimes are used without clear distinction. The ellipticity is not only usually defined as $\tan|\chi|$ but has also been extended to $\tan(\chi)$ to include the handedness of an ellipse. We prefer the term of ellipticity angle to denote the auxiliary angle χ.
[19] J. J. Krebs, B. T. Jonker, and G. A. Prinz, J. Appl. Phys. **61**, 2596 (1987).
[20] S. A. Haque, A. Matsuo, Y. Yamamoto, and H. Hori, J. Magn. Magn. Mater. **247**, 117 (2002).
[21] K. Baberschke and M. Farle, J. Appl. Phys. **81**, 5038 (1997).
[22] Y. Liu, Ph.D. thesis, Salford University, 2005.

AUTHOR QUERIES — 005618JAP

#1 Au: Please check deletions in eq. 8.
#2 Au: Please check insertion with respect to deletion in Eq. (8).
#3 Au: Please check changes and if meaning is presented
#4 Au: Please check deletions in Eq. (9)
#5 Au: Please check insertions with respect to deletion in Eq. (9).
#6 Au: Please check deletions in Eq. (21).
#7 Au: Please check insertions with respect to deletion in Eq. (21).
#8 Au: Please check
#9 Au: Please supply the city and publisher and city in Refs. 10 and 11, respectively
#10 Au: Please supply the city and publisher and city in Refs. 10 and 11, respectively